

Original Article

miR-206 inhibits cell biology of human glioblastoma by targeting MET

Bo Wang^{1,2}, Xiangmei Bu³, Qi Zhang², Chao Xu², Jinlong Sun¹, Zefu Li²

¹Department of Neurosurgery, Shandong Provincial Qianfoshan Hospital, Shandong University, Jinan, Shandong, PR China; Departments of ²Neurosurgery, ³Anesthesiology, Affiliated Hospital of Binzhou Medical College, Binzhou, Shandong, PR China

Received September 15, 2016; Accepted September 28, 2016; Epub November 1, 2016; Published November 15, 2016

Abstract: In recent years, it has been reported that miRNA has been involved in the progression and development of some malignant tumors. The expression model and action mechanisms of miR-206 have not yet been reported in human glioblastoma (GBM). In the present study, we carried out miRNA mimics transfection, immunoblotting, and RT-PCR et al to investigate the function of miR-206 in GBM tissues and cells. In this work, our team identified that the expression of miR-206 was decreased in GBM tissues and cells, but increased in paired non-cancer tissues and NHA cells (all $P < 0.001$). In addition, the expression level of MET mRNA and protein was increased in GBM tissues and cell lines (all $P < 0.001$). Functionally, the ectopic miR-206 expression inhibited GBM cell proliferation, motility and invasiveness. Mechanically, we demonstrated that the 3' untranslated regions (3'-UTR) of MET was a bona-fond target of miR-206, and overexpressed miR-206 affected the post-transcription expression of MET protein in GBM cells. At the same time, ectopic miR-206 expression decreased the expression of EGFR, Bcl-2 and MMP2/9, and promoted the expression of Bax protein. In conclusion, miR-206 inhibits cell proliferation, migration and invasion by targeting 3'-UTR of MET in the development of GBM, thus miR-206 can serve as a tumor suppressor via targeting MET in the treatment of GBM. Therefore, miR-206-MET signals could be recommended as a potential target for treatment of GBM.

Keywords: miR-206, MET, GBM

Introduction

Astrocytomas are derived from astrocytes in human central system, and act as the most common type of brain neoplasms, accounting for about 70% of all primary brain tumors [1, 2]. Histologically, the World Health Organization (WHO) divided astrocytomas into four histological malignancy grades [3, 4], among which grade IV astrocytoma, also called as GBM, is the most aggressive in all gliomas, accounting for about 55% of all astrocytomas [5, 6]. The overall survival time of GBM patients was changed greatly in recent decades, and most patients developed into the disease recurrence and progression in one year. Thus it is essential to hunt for biomarkers to better diagnostic, prognostic and therapeutic status for patients with astrocytomas, especially with GBMs.

MiRNA is a kind of non-coding RNAs, consisting of 19~25 nucleotides, and modulates post-

transcription of relevant genes by binding the 3'-UTR of target mRNAs, and then led to degradation of mRNA or inhibition of translation [7]. In most tumors of human, miRNAs can act as an oncogene or tumor suppressor to repress translation or induce degradation of mRNA [8]. Previous reports identified that the expression of miR-206 is decreased and recommended as a prognostic biomarker in many types of tumors and malignancies, including colorectal cancer, ovarian cancer, gastrointestinal stromal tumor, and squamous cell carcinoma in head and neck [9-14]. Recently, it was reported that the expression of miR-206 was obviously decreased in GBM samples, and the expression was associated with the pathological grade, indicating the potential tumor-suppressing role of miR-206 in GBM. However, the role of miR-206 in tumorigenesis of GBM is still unknown.

In the present study, we investigated the expression level of miR-206, and then explore the

role of miR-206 in the proliferation, migration and invasion in GBM cell lines, and then demonstrated their anticancer effects. At the same time, we also assessed whether miR-206/MET pathway could be potential targets for GBM therapy.

Materials and methods

Ethics statement

The present study was approved by the Ethics Committee of Shandong Provincial Qianfoshan Hospital, Shandong University. Patients enrolled in this study signed written informed consent. All procedures were subjected to the Declaration of Helsinki.

Patients and tissues

We selected 30 cases of fresh GBM tissues derived from GBM patients at Shandong Provincial Qianfoshan Hospital, Shandong University. A part of GBM tissues were preserved and sliced into paraffin sections just for pathologic diagnosis according to the WHO standard by two established neuropathologists, when differences occurred, the problems can be resolved by their careful review and discussion. And the tissues left were snap-frozen in liquid nitrogen, and then kept in the fridge at -80°C for the extraction of RNA and other assays. Prior to RNA extraction from frozen tissues, the relevant tumor samples were subjected to frozen sections, and then the sections were analyzed and reviewed by a neuropathologist to make sure that a minimum of 80% of cancer cells can be included in GBM tissues. For GBM patients, none of them had chemotherapy or radiotherapy prior to treatment. Finally, patients must be excluded from our study if patients died of conditions not related to GBM.

Cell culture

Regarding cell culture, primary normal human astrocytes (NHA) were purchased from the ScienCell Research Laboratories (Carlsbad, CA) and cultured under the conditions as instructed by the instructions. Human GBM cell lines U87 and U251 were obtained from the KeyGEN Company (China) and cultured in DMEM, 10% fetal bovine serum (Gibco, Grand Island, NY, USA) and 1% penicillin-streptomycin (Gibco,

Grand Island, NY, USA) at 37°C in a humidified atmosphere under 5% CO_2 . The medium was replaced every 3 days.

qRT-PCR

Total RNA containing miRNA was extracted from cultured cells or tissues using miRNeasy Mini Kit (Qiagen). cDNA was synthesized using miScript Reverse Transcription Kit (Qiagen) following the manufacturer's instructions. Reverse transcription was undertaken using 50 ng total RNA with a primer specific for miR-206, together with the SYBR Green microRNA reverse transcription kit. miRNAs were quantified using the SYBR Green miRNA qRT-PCR assay according to the manufacturer's protocol (Applied BioSystems). The qRT-PCR reaction was carried out on a 7500 Fast Real-time System (Applied Biosystems). All quantitative RT-PCRs were performed in triplicate. The data were analyzed using an automated baseline. The threshold cycle (Ct) was defined as the fractional cycle number at which the fluorescence exceeded the given threshold. The data obtained from the qRT-PCR were analyzed using the $\Delta\Delta\text{Ct}$ method ($2^{\Delta\Delta\text{Ct}}$). The PCR primers sets used here for miR-206 was designed as follows: miR-206 forward primer: 5'-TGGA-GACTTCTGAACGAGAG-3', and reverse primer: 5'-CTTGAAGATGGCGTTGGG-3'. U6 was used as an internal control and amplified with forward primer: 5'-GCTTCGGCAGCACATATACTAAAAT-3', and reverse primer: 5'-CGCTTCACGAATTTGCG-TGTCAT-3'. human MET forward primer: 5'-CT-CCTGGGGATGTGTAATGG-3' and reverse 5'-GC-CTCCATGGCATAACATAGG-3'; human GAPDH forward primer: 5'-GGGCATCCTGGGCTACTG-3' and reverse 5'-GAGGTCCACCACCCTGTTGC-3'.

Transient transfection of miR-206 oligonucleotides

Cells were transiently transfected with 50 nmol of the miR-206 mimic with Lipofectamine 2000 (Invitrogen) according to the manufacturer's recommendation. The antisense oligonucleotides used in these studies were the miR-206 primer as mentioned above; the miRNA mimic-negative control (NC mimic): 5'-UUCUCC-GAACGUGUCACGUTT-3' and 5'-ACGUGACAG-UUCGGAGAATT-3'. All miRNA oligonucleotides were purchased from Genepharma (Shanghai, China).

Western blot analysis

For the protein analysis, the cells were harvested at 12~24 h following different treatments, as described above, and washed with cold PBS and then incubated in ice-cold RIPA buffer. Cell lysates were sonicated for 30 s on ice and lysed at 4°C for 60 min. Then, the cell lysates were centrifuged at 12,000 g for 30 min at 4°C. Protein concentrations in the supernatants were determined by the BCA reagent. Total protein was separated by denaturing 8-12% SDS-polyacrylamide gel electrophoresis, which was resolved over and electrotransferred by semidry blotting (Bio-Rad Laboratories, Shanghai) onto a nitrocellulose membrane. The membrane was incubated with primary antibodies (Abcam, Cambridge, UK, 1:1000 dilution) or β -actin (Santa Cruz Biotech, Santa Cruz, CA, 1:1000 dilution) overnight at 4°C, and then with peroxidase-conjugated secondary antibody (Santa Cruz Biotech, Santa Cruz, CA, 1:1000 dilution), visualized by chemiluminescence (GE, Fairfield, CT, USA).

Cell proliferation assay

Cells were seeded at 2,000 per well in 96-well plates and cultured after transfection. Cell proliferation was detected at the indicated time points using a CCK-8 kit (Dojindo Laboratories) following the manufacturer's instructions. All assays were performed in octuplicate and repeated at least three times.

Wound-healing assay

Cells were seeded in 12-well plates and grown to 90% confluence. Cells were transfected with or without NC miRNAs or miR-206 mimics. After 36 h of transfection, cells were serum starved overnight and a linear wound was created using a pipette tip. Wound closure was monitored using live cell imaging microscopy at an interval of 30 min for 24-48 h. Wound size was then measured randomly at three sites perpendicular to the wound.

Transwell invasion assays

As for transwell assay, we seeded cells on the upper chamber of each insert, and then, 500 μ l of DMEM (10% FBS) was added to a 24-well plate for 12 hour incubation at 37°C, the cells on the lower layer were collected, and fixed with a 0.1% crystal violet. As for invasion

assay, transwell chambers were uniformly plated with 60 μ l Matrigel diluted with DMEM, and then incubated for 4 h at 37°C, and then the same procedures with migration assay were conducted.

Luciferase reporter assay

A dual-luciferase reporter vector was used to generate the luciferase constructs. The target genes of miR-206 were selected based on target scan algorithms [microRNA.org (<http://www.microRNA.org/microRNA/home.do>) Microcosm (<http://www.ebi.ac.uk/enright-srv/microcosm/htdocs/targets/>) and TargetScan (<http://www.targetscan.org/>)]. For 3'UTR luciferase assay, the putative binding sites of miR-206 and its homologous mutation sites in the 3'-UTR region of MET mRNA were amplified and cloned into pGL3-contra luciferase reporter plasmid (Invitrogen, Carlsbad, CA). The pRL vector constitutively expressing Renilla luciferase was used to normalize for transfection efficiency. Luciferase activity was measured using the Dual-Luciferase Reporter Assay System (Promega, Madison, USA) after transfection at 48 h. Data are presented as the mean value \pm standard deviations (SD) for triplicate experiments.

Statistical analysis

Significance was determined using the one-way ANOVA test on the mean values of three different experiments. Significance was determined using the mean \pm SD and was analyzed by 2-tailed Student's t-tests using the Statistical Program for Social Sciences 13.0 software (SPSS Corp., Shanghai, China). $P < 0.05$ was used as the cutoff for statistically significant differences. In the Western blotting analysis, the corresponding strips used to estimate the value of the relative protein content were captured photographically through a Bio-Rad image analysis system with Image-Pro software analysis.

Results

The expression profile of miR-206 and MET in GBM samples

In this work, our team detected the expression of miR-206 and MET in 30 pairs of tumor tissues and adjacent normal tissues, and then we found that the expression of miR-206 was obvi-

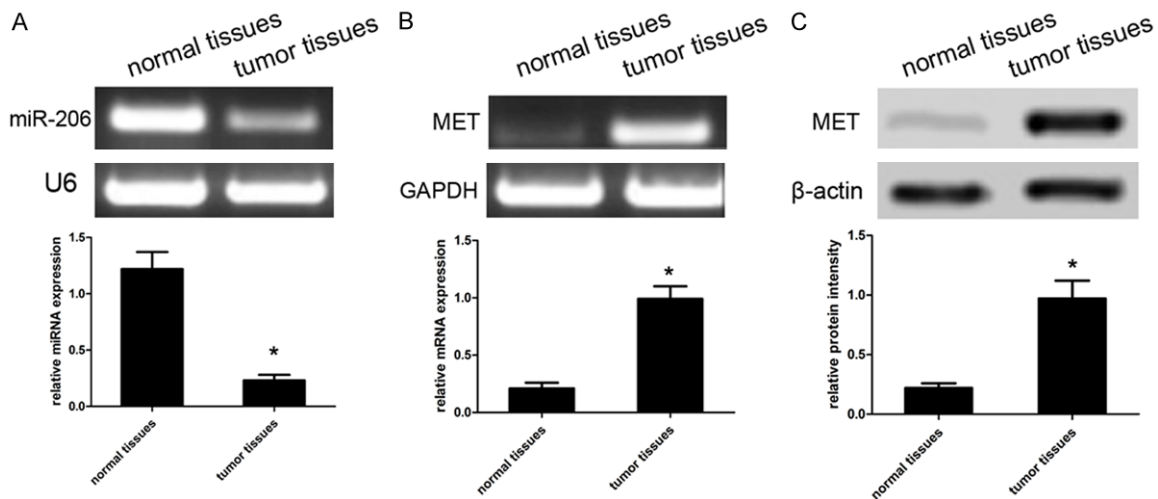


Figure 1. The expression profile of miR-206 and MET in GBM tissues. A, B. The RT-PCR analysis of miR-206 and MET mRNA expression were conducted in tumor tissues and matched non-tumor tissues. Quantification analysis was defined as the relative density of miR-206 and MET mRNA to U6 and GAPDH, respectively. U6 or GAPDH was used as an internal control. Results shown are the mean \pm SD of repeated independent experiments. * $P < 0.001$, compared with normal tissues, one-way ANOVA. C. The expression of MET protein was examined in tumor tissues and matched non-tumor tissues using western blot. The average MET protein expression was normalized to β -actin. Results shown are the mean \pm SD of repeated independent experiments. * $P < 0.001$, compared with normal tissues, one-way ANOVA.

ously higher in tumor tissues than that in paired normal tissues ($P < 0.001$; **Figure 1A**). Subsequently, we detected the expression of MET and found that the mRNA expression of MET was greatly increased in tumor tissues than that in paired normal tissues ($P < 0.001$; **Figure 1B**). On the other hand, the protein expression of MET was also obviously increased in tumors than that in normal tissues ($P < 0.001$; **Figure 1C**). In general, the average optical density of bands of MET mRNA and protein in all 30 cases of tissues is 0.88 ± 0.13 , and 1.11 ± 0.12 , respectively, which is significantly different from that in normal tissues (0.32 ± 0.05 , and 0.33 ± 0.06 , respectively).

The expression profile of miR-206 and MET in GBM cells

To further elucidate the role of miR-206 in the progression and development of GBM cells, our team tested the expression profile of miR-206 and MET in human GBM cell lines U87 and U251. In the present study, total RNA was extracted from U87 and U251 cells with different treatment, and then the expression levels of miR-206 and MET were subjected to qRT-PCR. Our findings showed that the expression level of miR-206 was obviously decreased in both U87 and U251 cell lines, but the expres-

sion level of miR-206 was obviously increased in control human NHA cells ($P < 0.001$; **Figure 2A**). At the same time, the expression level of MET mRNA was markedly up-regulated in both U87 and U251 cells instead of NHA cells ($P < 0.001$; **Figure 2B**). What is more, the expression level of MET protein was also increased in either U87 or U251 cells in comparison with control NHA cells ($P < 0.001$; **Figure 2C**).

Effects of miR-206 on GBM cell proliferation

To elucidate the impact of miR-206 on GBM cell proliferation, we transfected U87 and U251 cells with miR-206 mimic or miR-NC, and then U87 and U251 cells were subjected to CCK-8 assay. We found that U87 and U251 cells transfected with miR-206 mimics significantly decreased the cell growth of U87 and U251 cells in comparison with control miR-NC ($P < 0.001$; **Figure 3A**), suggesting that the proliferation of U87 and U251 cells was significantly affected owing to ectopic miR-206 expression. Using immunoblotting, our team detected the cell proliferation-corresponding proteins, including EGFR, Bcl-2 and Bax. Consistent with CCK-8 assay, our team found that the expression of EGFR and Bcl-2 was significantly down-regulated in U87 and U251 cells transfected with miR-206 mimics, when compared

miR-206 and MET

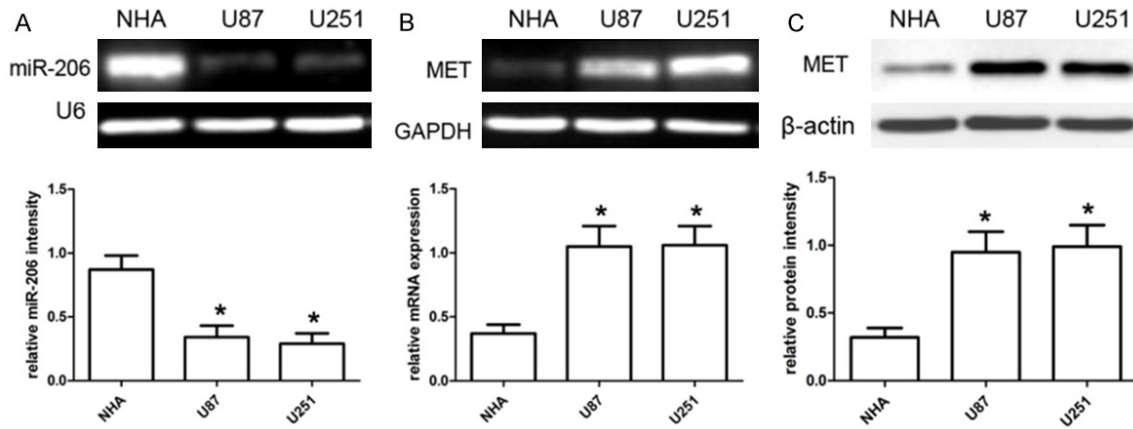


Figure 2. The expression profile of miR-206 and MET in GBM cell lines. A, B. RT-PCR analysis of miR-206 and MET expression in glioblastoma U87 and U251 cell lines. Quantification analysis was defined as the relative density of miR-206 and MET mRNA to U6 and GAPDH respectively. U6 or GAPDH was used as an internal control. Results shown are the mean \pm SD of repeated independent experiments. * $P < 0.001$, compared with NHA cells, one-way ANOVA. C. The expression of MET protein was examined in GBM cell lines U87 and U251 using western blot. The MET expression was normalized to β -actin expression. Results shown are the mean \pm SD of repeated independent experiments. * $P < 0.001$, compared with NHA cells, one-way ANOVA.

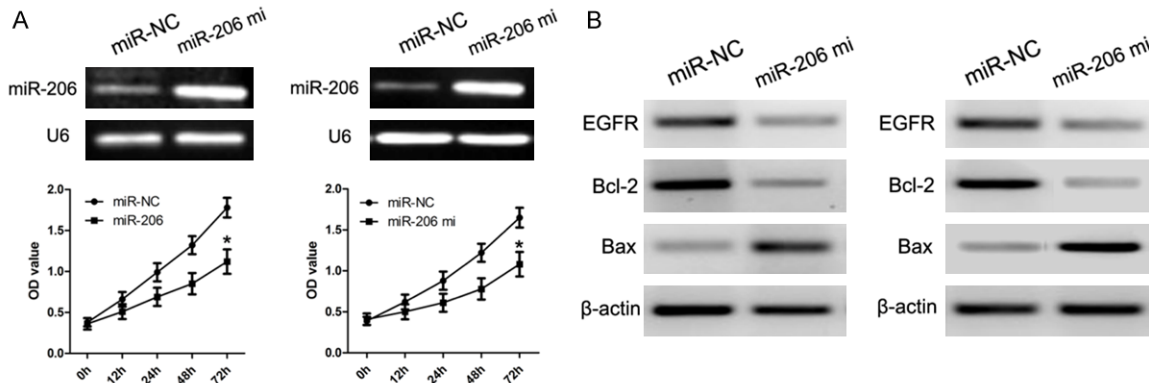


Figure 3. miR-206 inhibits glioblastoma cell proliferation. A. Cells were transfected with miR-206 mimics and identified by RT-PCR. Cell proliferation was measured using a CCK-8 assay. U87 and U251 cells were transfected with miR-206 mimics or scramble control miRNAs. B. Relative EGFR, Bcl-2 and Bax expression in U87 and U251 cells was measured after the cells were transfected with miR-206 mimics or NC miRNA using western blot. Results shown are the mean \pm SD of repeated independent experiments. * $P < 0.001$, compared with miR-NC, one-way ANOVA.

with cells with miR-NC control (**Figure 3B**). On the other hand, the protein expression of Bax was increased in U87 and U251 cells transfected with miR-206, when compared with miR-NC control (**Figure 3B**). These findings indicated that ectopic miR-206 expression affected U87 and U251 cell proliferation.

Effects of miR-206 on GBM cell migration and invasion

To figure out the effect of miR-206 on GBM cell migration and invasion, we carried out the

wound healing and transwell assays using U87 and U251 cells treated with miR-206 mimics or miR-NC. Through the wound healing assay, our results showed that ectopic miR-206 expression could affect U87 and U251 cell migration when compared with miR-NC ($P < 0.001$; **Figure 4A**). In the transwell assay, ectopic miR-206 expression was able to decrease U87 and U251 cell invasion number when compared with miR-NC ($P < 0.001$; **Figure 4B**). Based on molecule level, our team applied western blot to evaluate the expression of proteins related to cell invasion, and observed that the expres-

miR-206 and MET

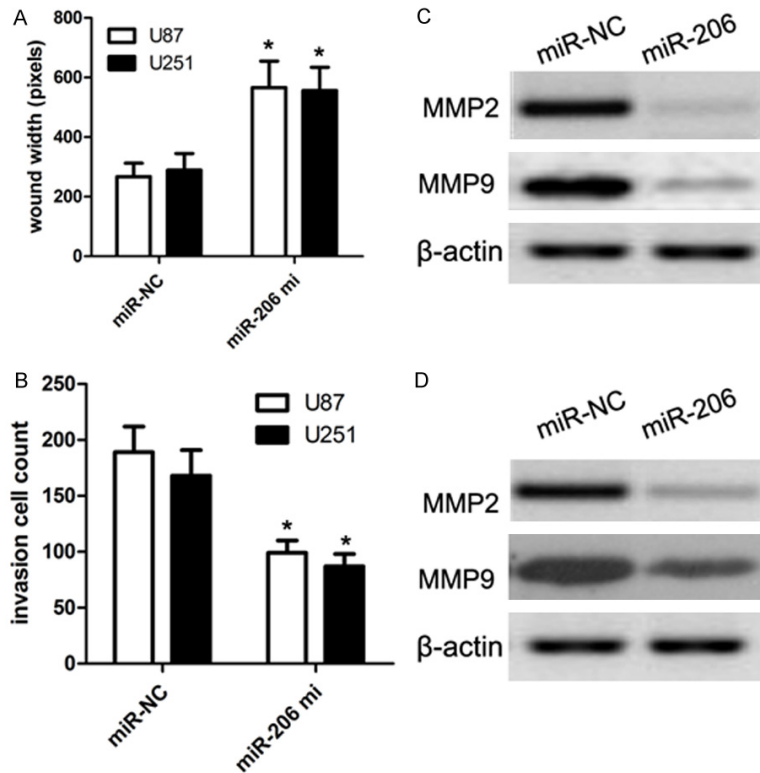


Figure 4. miR-206 reduces GBM cell migration and invasion. A. Wound healing assay performed with U87 and U251 cells over 48 h. Cells and wounds were pretreated as described above. Wound healing within the scrape line was recorded every day. Representative scrape lines are shown at day 3; dashed line indicates the margin of the scratch at day 1. B. Representative fields ($\times 10$ magnification) showing invasive cells after 24 hour culture in Matrigel invasion chambers. Panels show U87 and U251 cell invasion after transfection with miR-206 mimics or miR-NC. Quantitative analysis of cell invasion experiments demonstrates that miR-206 decreases U87 and U251 cell invasion compared to miR-NC ($*P < 0.001$, vs. miR-NC control). C. Relative MMP2/9 expressions in U87 cells were measured after the cells were transfected with miR-206 mimics or miR-NC using western blot. D. Relative MMP2/9 expressions in U251 cells were measured after the cells were transfected with miR-206 mimics or miR-NC using western blot. Results shown are the mean \pm SD of repeated independent experiments. $*P < 0.001$, compared with miR-NC, one-way ANOVA.

sion of MMP2 and MMP9 protein was obviously decreased in U87 and U251 cell lines transfected with miR-206 mimics, but the expression of MMP2 and MMP9 protein was significantly increased in the miR-NC-treated GBM cell lines ($P < 0.001$; **Figure 4C**). These observations indicated that ectopic miR-206 exerts the inhibitory effects on GBM cell migration and invasion.

miR-206 directly targets the 3'-UTR of MET

In this work, we found that miR-206 may directly target the 3'-UTR of MET, and then inhibits the post-translation processed of MET based

on three miRNA databases. In order to identify the direct relationship between miR-206 and MET, we used the TCGA dataset to demonstrate that the inverse association between miR-206 and MET ($P < 0.0001$). To determine whether miR-206 directly targets the 3'-UTR of MET mRNA, our team cloned a full-length 3'-UTR (wt/mut) of MET mRNA, and inserted them into a luciferase reporter vector with downstream from the firefly luciferase gene. After that, the protein level of MET was also measured in the GBM cell lines using the western blot. We observed that ectopic miR-206 expression seriously decreased the luciferase activity of cells with MET-3'-UTR-wt in a consistent and dose-dependent manner (**Figure 5A**). Conversely, ectopic miR-206 expression did not decrease the luciferase activity of cell with MET-3'-UTR-mut (**Figure 5B**). Our findings identified that the expression level of MET protein was reduced in cells transfected with the miR-206 and 3'-UTR-wt, when compared to the negative control miR-NCs. However, the expression of MET protein in the cells transfected with miR-206 and MET 3'-UTR-mut

showed the same expression model with its negative control. These findings suggested that the 3'-UTR of MET is a direct miR-206, by which miR-206 affected the post-translation expression of MET, resulting in dysfunction of cell function.

Discussion

Recently, the expression of MET has been found on multiple solid tumors as well as hematological malignancies. Growing evidence has accumulated that the MET pathway plays an important role in multiple processes such as

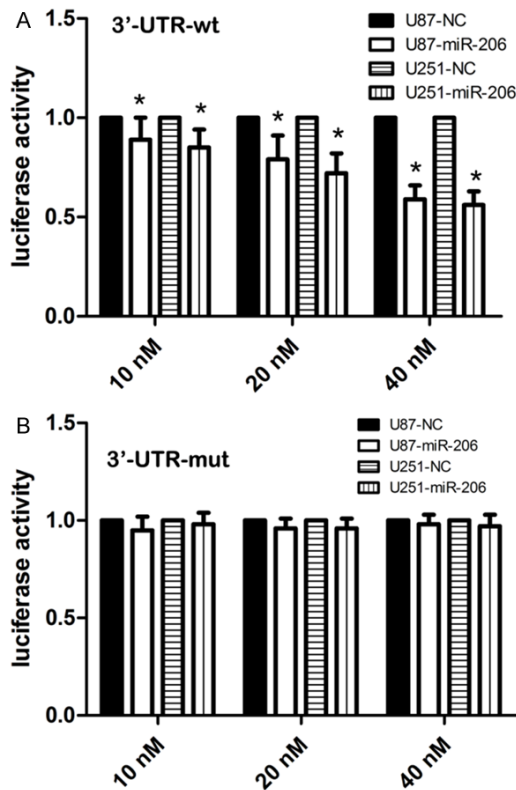


Figure 5. MET is a candidate target of miR-206. The miR-206 mimic inhibited the luciferase activity controlled by wild-type MET-3'-UTR (A) but did not affect the luciferase activity controlled by mutant MET-3'-UTR (B) in U87 and U251 cells. Results shown are the mean \pm SD of repeated independent experiments. * $P < 0.001$, compared with miR-NC, one-way ANOVA.

stem cell mobilization, migration and homing, inflammation, infection and immunoregulation. The mechanisms employing the MET have been also implicated in tumor development, growth and metastasis [15-17]. There is increasing evidence showing dysfunction of the MET links to the pathogenesis of cancer. Besides, the disruption of MET has been reported to be involved into the initiation and development of human GBM. As reported, the down-regulation of miRNAs can triggers oncogenesis via regulating oncogenes or silencing tumor suppressor genes. miR-206 is downregulated in human breast cancer [18]. In the context of GBM, aberrant expression of specific miRNAs are closely associated with tumour cell proliferation, migration and invasion by targeting proteins involved in these cellular functions. However, the expression and the role of miR-206 in GBM have not been clearly demonstrated.

Our tissues analysis showed that the expression of miR-206 was obviously decreased in tumor tissues than that in paired normal tissues. Besides, the mRNA and protein level of MET revealed higher expression in tumor tissues than normal tissues. Our results were consistent with previous findings, which indicated that the expression of miR-206 was obviously downregulated in human breast cancer tissues [18]. Recent reports also indicated that ectopic miR-206 expression plays a suppressor role in the cell proliferation, migration and invasion of tumors. Most importantly, our bioinformatics indicated that the tumor-suppressing effects of miR-206 depend on its regulation of MET translation. Based on the previous study, this will be the first study to elucidate the role of miR-206 in post-transcriptional regulation of MET in GBM cells.

Recent data indicates that increased expression of EGF and its receptor EGFR in gastric mucosa may induce changes in gastric epithelial cells leading to tumorigenesis [19, 20]. EGF, through interaction with its receptor, stimulates the cell proliferation and migration and triggers epithelial cell signaling [21]. Besides, matrix metalloproteinases are secreted during the growth, invasion, metastases, and angiogenesis of tumors, and can affect the surrounding microenvironment, causing dynamic changes of biological behaviors of the tumor [22-25]. However, the precise molecular mechanisms between EGFR and MMP2/9 in the cellular malignant and invasive phenotypes are not fully understood. In the present study, we found that cells transfected with miR-206 decreased the expression of EGFR protein, while the miR-NC unfazed the expression of EGFR protein, which indeed showed that miR-206 decreased GBM cell proliferation. At the same time, we also found that cells transfected with miR-206 decreased the expression of MMP2/9 protein, whereas the control miR-NC promoted the protein expression of MMP2/9. These findings suggested that ectopic miR-206 expression exerts the inhibitory effects on GBM cell migration and invasion.

Emerging evidence demonstrated the relationships between the MET and angiogenesis in the development of tumors by the increase of VEGF or VEGFR, which serves as the most potent proangiogenic factors [26]. The MET has been recommended as a potential treatment

target for anticancer therapeutics [27]. Till now, more than 15 kinds of new drugs targeting the MET have been developed worldwide, and have been approved for use in patients with non-Hodgkin's lymphoma and multiple myeloma, by the Food and Drug Administration [28]. These advances promote the therapeutic application of the MET pathway against GBM. Thus, miR-206 may be used to target the MET pathway to treat GBM patients.

In conclusion, this study suggested that the expression of miR-206 and MET may be predictive of worse clinical outcome in patients with GBM. Our findings also highlight the therapeutic potential of miR-206/MET pathway in GBM patients, and support the development of effective therapeutic strategies that target miR-206 or MET by a pharmacological approach.

Acknowledgements

This work was supported by the Foundation of Binzhou Medical College (BY2015KJ19).

Disclosure of conflict of interest

None.

Address correspondence to: Jinlong Sun, Department of Neurosurgery, Shandong Provincial Qianfoshan Hospital, Shandong University, Jinan 250-014, Shandong, PR China. E-mail: sunjlsdqfs@163.com; Zefu Li, Department of Neurosurgery, Affiliated Hospital of Binzhou Medical College, Binzhou 256603, Shandong, PR China. E-mail: lizefeifeis-hand@126.com

References

- [1] Yu J, Wang M, Song J, Huang D, Hong X. Potential Utility of Visually Accessible Rembrandt Images Assessment in Brain Astrocytoma Grading. *J Comput Assist Tomogr* 2016; 40: 301-6.
- [2] Frosina G. The glioblastoma problem: targeting by combined medicinal chemistry approaches. *Curr Med Chem* 2015; 22: 2506-24.
- [3] Lv Q, Zhang J, Yi Y, Huang Y, Wang Y, Wang Y, Zhang W. Proliferating Cell Nuclear Antigen Has an Association with Prognosis and Risks Factors of Cancer Patients: a Systematic Review. *Mol Neurobiol* 2015; [Epub ahead of print].
- [4] Lv B, Yang X, Lv S, Wang L, Fan K, Shi R, Wang F, Song H, Ma X, Tan X, Xu K, Xie J, Wang G, Feng M, Zhang L. CXCR4 Signaling Induced Epithelial-Mesenchymal Transition by PI3K/AKT and ERK Pathways in Glioblastoma. *Mol Neurobiol* 2015; 52: 1263-8.
- [5] Altieri R, Fontanella M, Agnoletti A, Panciani PP, Spena G, Crobeddu E, Pilloni G, Tardivo V, Lanotte M, Zenga F, Ducati A, Garbossa D. Role of Nitric Oxide in Glioblastoma Therapy: Another Step to Resolve the Terrible Puzzle? *Transl Med Uni Sa* 2014; 12: 54-9.
- [6] De Paepe A, Vandeneede N, Strens D, Specenier P. The Economics of the Treatment and Follow-Up of Patients with Glioblastoma. *Value Health* 2015; 18: A448.
- [7] Farazi TA, Spitzer JI, Morozov P, Tuschl T. miRNAs in human cancer. *J Pathol* 2011; 223: 102-115.
- [8] Croce CM, Calin GA. miRNAs, cancer, and stem cell division. *Cell* 2005; 122: 6-7.
- [9] Zhou J, Tian Y, Li J, Lu B, Sun M, Zou Y, Kong R, Luo Y, Shi Y, Wang K, Ji G. miR-206 is down-regulated in breast cancer and inhibits cell proliferation through the up-regulation of cyclinD2. *Biochem Biophys Res Commun* 2013; 433: 207-12.
- [10] Geisler A, Schön C, Größl T, Pinkert S, Stein EA, Kurreck J, Vetter R, Fechner H. Application of mutated miR-206 target sites enables skeletal muscle-specific silencing of transgene expression of cardiotropic AAV9 vectors. *Mol Ther* 2013; 21: 924-33.
- [11] Zhang L, Liu X, Jin H, Guo X, Xia L, Chen Z, Bai M, Liu J, Shang X, Wu K, Pan Y, Fan D. miR-206 inhibits gastric cancer proliferation in part by repressing cyclinD2. *Cancer Lett* 2013; 332: 94-101.
- [12] Wu J, Yang T, Li X, Yang Q, Liu R, Huang J, Li Y, Yang C, Jiang Y. Alteration of serum miR-206 and miR-133b is associated with lung carcinogenesis induced by 4-(methylnitrosamino)-1-(3-pyridyl)-1-butanone. *Toxicol Appl Pharmacol* 2013; 267: 238-46.
- [13] Yan B, Zhu CD, Guo JT, Zhao LH, Zhao JL. miR-206 regulates the growth of the teleost tilapia (*Oreochromis niloticus*) through the modulation of IGF-1 gene expression. *J Exp Biol* 2013; 216: 1265-9.
- [14] Jalali S, Ramanathan GK, Parthasarathy PT, Aljubran S, Galam L, Yunus A, Garcia S, Cox RR Jr, Lockey RF, Kolliputi N. Mir-206 regulates pulmonary artery smooth muscle cell proliferation and differentiation. *PLoS One* 2012; 7: e46808.
- [15] Shuch B, Falbo R, Parisi F, Adeniran A, Kluger Y, Kluger HM, Jilaveanu LB. MET Expression in Primary and Metastatic Clear Cell Renal Cell Carcinoma: Implications of Correlative Biomarker Assessment to MET Pathway Inhibitors. *Biomed Res Int* 2015; 2015: 192406.
- [16] Matsusaka S, Kobunai T, Yamamoto N, Chin K, Ogura M, Tanaka G, Matsuoka K, Ishikawa Y, Mizunuma N, Yamaguchi T. Prognostic impact

miR-206 and MET

- of KRAS mutant type and MET amplification in metastatic and recurrent gastric cancer patients treated with first-line S-1 plus cisplatin chemotherapy. *Genes Cancer* 2016; 7: 27-35.
- [17] Park S, Langley E, Sun JM, Lockton S, Ahn JS, Jain A, Park K, Singh S, Kim P, Ahn MJ. Low EGFR/MET ratio is associated with resistance to EGFR inhibitors in non-small cell lung cancer. *Oncotarget* 2015; 6: 30929-38.
- [18] Lee ST, Chu K, Jung KH, Kim JH, Huh JY, Yoon H, Park DK, Lim JY, Kim JM, Jeon D, Ryu H, Lee SK, Kim M, Roh JK. miR-206 regulates brain-derived neurotrophic factor in Alzheimer disease model. *Ann Neurol* 2012; 72: 269-77.
- [19] García I, Vizoso F, Andicoechea A, Fernandez P, Suarez C, García-Muñoz JL, Allende MT. C-erbB-2 oncoprotein content in gastric cancer and in adjacent mucosa. *Int J Biol Markers* 2000; 15: 231-4.
- [20] Dan L, Jian D, Na L, Xiaozhong W. Crosstalk between EGFR and integrin affects invasion and proliferation of gastric cancer cell line, SGC7901. *Onco Targets Ther* 2012; 5: 271-7.
- [21] Chen W, Zhong X, Wei Y, Liu Y, Yi Q, Zhang G, He L, Chen F, Liu Y, Luo J. TGF- β Regulates Survivin to Affect Cell Cycle and the Expression of EGFR and MMP9 in Glioblastoma. *Mol Neurobiol* 2016; 53: 1648-53.
- [22] Kessenbrock K, Plaks V, Werb Z. Matrix metalloproteinases: regulators of the tumor microenvironment. *Cell* 2010; 141: 52-67.
- [23] Yang X, Lv S, Liu Y, Li D, Shi R, Tang Z, Fan J, Xu Z. The Clinical Utility of Matrix Metalloproteinase 9 in Evaluating Pathological Grade and Prognosis of Glioma Patients: A Meta-Analysis. *Mol Neurobiol* 2015; 52: 38-44.
- [24] Kumar B, Koul S, Petersen J, Khandrika L, Hwa JS, Meacham RB, Wilson S, Koul HK. p38 mitogen-activated protein kinase-driven MAPKAPK2 regulates invasion of bladder cancer by modulation of MMP-2 and MMP-9 activity. *Cancer Res* 2010; 70: 832-41.
- [25] Zhang Y, Du Z, Zhang M. Biomarker development in MET-targeted therapy. *Oncotarget* 2016; 7: 37370-37389.
- [26] Matsusaka S, Kobunai T, Yamamoto N, Chin K, Ogura M, Tanaka G, Matsuoka K, Ishikawa Y, Mizunuma N, Yamaguchi T. Prognostic impact of KRAS mutant type and MET amplification in metastatic and recurrent gastric cancer patients treated with first-line S-1 plus cisplatin chemotherapy. *Genes Cancer* 2016; 7: 27-35.
- [27] Takahashi N, Iwasa S, Taniguchi H, Sasaki Y, Shoji H, Honma Y, Takashima A, Okita N, Kato K, Hamaguchi T, Shimada Y, Yamada Y. Prognostic role of ERBB2, MET and VEGFA expression in metastatic colorectal cancer patients treated with anti-EGFR antibodies. *Br J Cancer* 2016; 114: 1003-11.
- [28] Rosenblat JD, Kakar R, Berk M, Kessing LV, Vinberg M, Baune BT, Mansur RB, Brietzke E, Goldstein BI, McIntyre RS. Anti-inflammatory agents in the treatment of bipolar depression: a systematic review and meta-analysis. *Bipolar Disord* 2016; 18: 89-101.